OPEN ACCESS

International
Journal
Of Modern Engineering Research (IJMER)

New Implementation of Dc-Dc Converter for Residential Microgrid System

P. Geetha[1], S. Jayanthi[2]

[1] *(P.G (PE&D) student, Department of EEE, Dhanalakshmi Srinivasan Engineering College, Perambalur-12)*
[2] *(Head of the department, Department of EEE, Dhanalakshmi Srinivasan Engineering College, Perambalur-12)*

***Abstract*:** *This paper proposes a integrated converter for interfacing between the energy storage system and the dc bus for a residential microgrid system. In this project dc-dc converter is incorporated as the DC-DC conversion stage for the grid connected system. Benefiting from its circuit simplicity and number of active devices the promising features such as high voltage ratio, high power operation on the discharging process, bidirectional power flow, low input and output current ripple. This converter uses one full bridge dc-dc converter and ac-ac converter to control and produce high voltage ratio. To control the inverter phase shift modulation is used. So the proposed converter is verified through numerical solution using mat lab.and experimental results of the proposed topology are presented.*

Index Terms: *DC bus interconnection, dc–dc converter, energy storage system, microgrid, power converter integration.*

I. Introduction

Electrical energy consumption has been increasing in recent years, and It has been essential to the increase of electric power generation. Distributed generation (DG) technologies have been gaining interest due to some benefits such as high reliability, high power quality, modularity, efficiency, reduced or absent emissions, security, and load management [1], [2]. However, the uncontrolled use of individual DG units can cause various problems thereby compromising their benefits [3], [4]. Difficulties in connecting these units directly to the bulky ac system due to their variable and intermittent power generation, voltage oscillation in the line to which the sources are connected, and protection issues are some of these problems. As an alternative to reduce such problems, the microgrid conceptthas been gaining more notoriety each day [5], [6]. Some advantages of the microgrids are the possibility to generate electric power with lower environmental impact and easier connection system efficiency

In the microgrid systems, the energy storage system is of great importance. It is responsible for supplying energy to the loads when the main sources are not capable during short periods of time and steady-state operation. The proposed residential microgrid energy storage system composed of a battery bank and a super capacitor bank has two main functions. The battery bank acts as a backup device due to its high energy density [10], providing energy under the steady-state condition when the other sources are not capable. The super capacitor bank acts as a quick discharge device due to its high power density [11], providing energy to the microgrid during transitory periods, mainly during the bio fuel generator start-up time. Consequently, due to the importance of the energy storage system, this paper focuses specifically on the dc power module of the microgrid energy storage system.

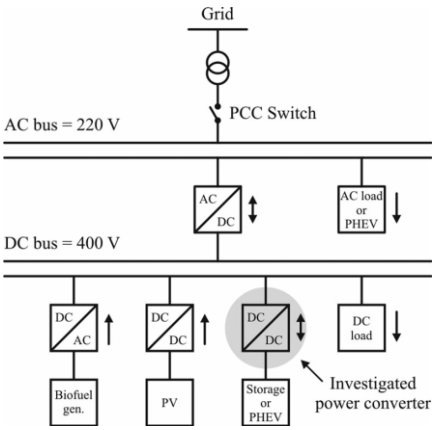

Figure.1.Residential microgrid system.

The dual active bridge (DAB) or modified DAB converters are approached in [12]–[20]. Papers [12] and [13] propose modulation schemes different from the conventional phase-shift modulation. In [12], a new hybrid modulation technique to expand the converter power range is proposed, while paper [13] proposes an optimal modulation scheme that enables minimum conduction and copper losses for a DAB converter. In [14], an input stage composed of a q ZSI converter is proposed, which guarantees the voltage boost during the super capacitor discharge, but increases the number of active switches. In [15], a DAB converter including unified soft-switching scheme (voltage clamp branch on the current-fed bridge) is proposed. Paper [16] discusses the steady-state operation of a phase-shift modulated dual-bridge series resonant converter. In [17], design issues of the DAB converter such as leakage inductance, switching frequency, and turns ratio are approached aiming for higher efficiency.

Paper [18] describes the design and performance of the converter and analyzes the effect of unavoidable dc-bias currents on the magnetic-flux saturation of the transformer. These topologies present high number of active devices and most of them present high input and output current ripple. Papers [21]–[27] regard different converter structures. In [21], a boost-dual -half -bridge converter is proposed applying phase shift modulation. Paper [22] proposes a three-port triple-half bridge bidirectional dc–dc converter, which comprises a high frequency three-winding transformer and three half-bridges.Topologies from [21] and [22] need six active switches and present low input current ripple, but high output current ripple.In [23], a converter composed of a full-bridge circuit on the primary side and a current-fed push–pull circuit on the secondary side is proposed. This topology needs six or eight active switches and a high number of additional components, presents high input current ripple, and the voltage over the output switches is twice the transformer output voltage. Paper [24] applies a half-bridge current source converter that needs only four active switches, but presents high input current ripple. Topology presented in [25] has a particular configuration, in which the supercapacitor bank is situated between two dc–dc converters that connect another energy source to the load. Paper [26] applies a full-bridge with active clamping and a half-bridge converter, but uses batteries and fuel cells. These last two topologies present eight and seven active switches, respectively, and both present high output current ripple.

II. Proposed Integrated Full-Bridge-Forward Dc–Dc Converter

The proposed converter must be designed for both charging and discharging processes. The maximum designed power for the microgrid energy storage system discharging process is equal to 1.4 kW (high power during transitories), which is supplied by the supercapacitor bank. The isolated static power converter traditionally used in applications with this power level (above 1 kW) is the full-bridge converter. The charging process of the microgrid energy storage system does not need to be performed with the same power level of the discharging process. Once the energy storage system of a residential microgrid is not often demanded due to the low electric energy supply interruption indices, there is a long period of time available between two interactions. This way, the charging process can have a longer duration and, consequently, be performed with lower power levels. Therefore, it is not necessary to use another full-bridge converter for the charging process. Due to the presence of the full-bridge converter for the discharging process, it is possible to utilize the respective active switches to rectify the converter output voltage during the charging process. This way, it is necessary to add only the input stage of the respective converter for the charging process. One of the simplest converters for this application is the forward converter, which demands only one active switch and is appropriate for the related power levels.

Therefore, the proposed dc–dc converter is the integration of a full-bridge and a forward converter. Full-bridge converter is responsible for the energy storage system discharging stage, while the forward converter is responsible for the energy storage system charging stage. This forward converter resultant by the integration process is called double ended forward converter. Moreover, other advantages are that it provides the use of a transformer turns ratio (tertiary higher than secondary) that avoids the circulation of reactive energy during the charging process, and the storage system voltage can be reduced without penalizing the full-bridge converter operation, once its input voltage is kept constant. During the energy storage system discharging stage, the bidirectional converter boosts the voltage from the energy storage system to an intermediate level, while during the energy storage system charging stage, it performs voltage postregulation or remains with *S*bid1 ON and *S*bid2 OFF acting as a low-pass filter, thus eliminating the switching losses.

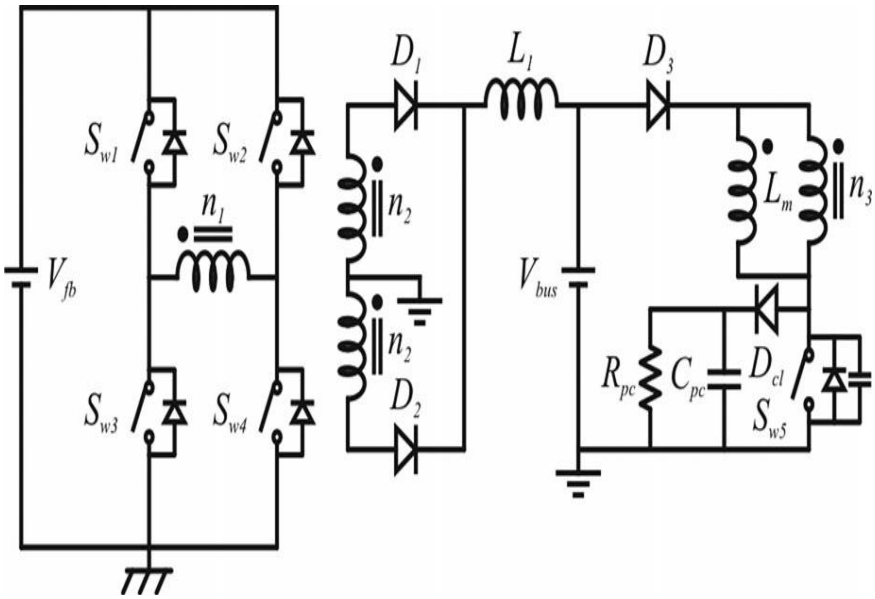

Figure.2: DAB including bidirectional converter

TABLE II
CONVERTER PARAMETERS

Parameter	Symbol	Value
DC bus voltage	V_{bus}	400 V
Full-bridge charging voltage	V_{charg}	50 to 55 V
Full-bridge discharging voltage	V_{fb}	80 V
Nominal storage system voltage	V_{sto}	48 V
Minimum storage system voltage	V_{sto_min}	24 V
Maximum forward switch voltage	V_{Sw5_max}	1200 V
Nominal charging power	P_{ch}	100 W
Maximum discharging power	P_{disch}	1.4 kW

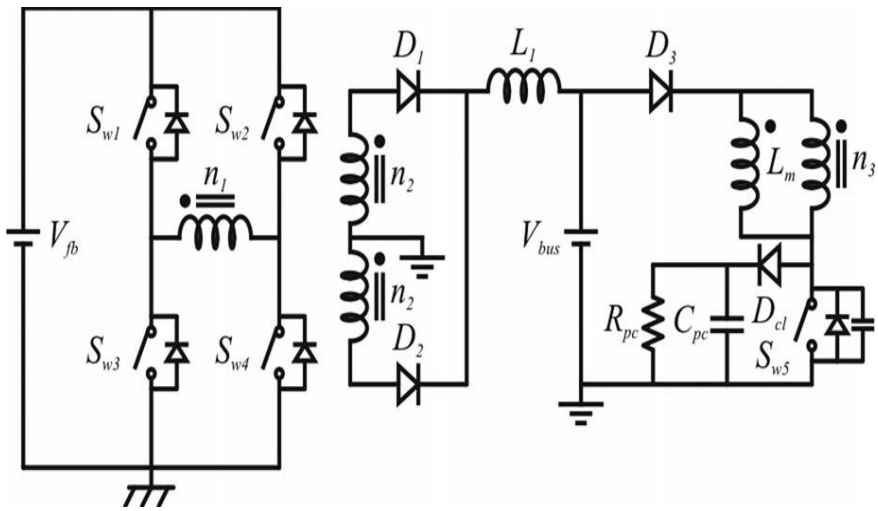

Figure. 3: Proposed converter with dissipative passive clamping circuit.

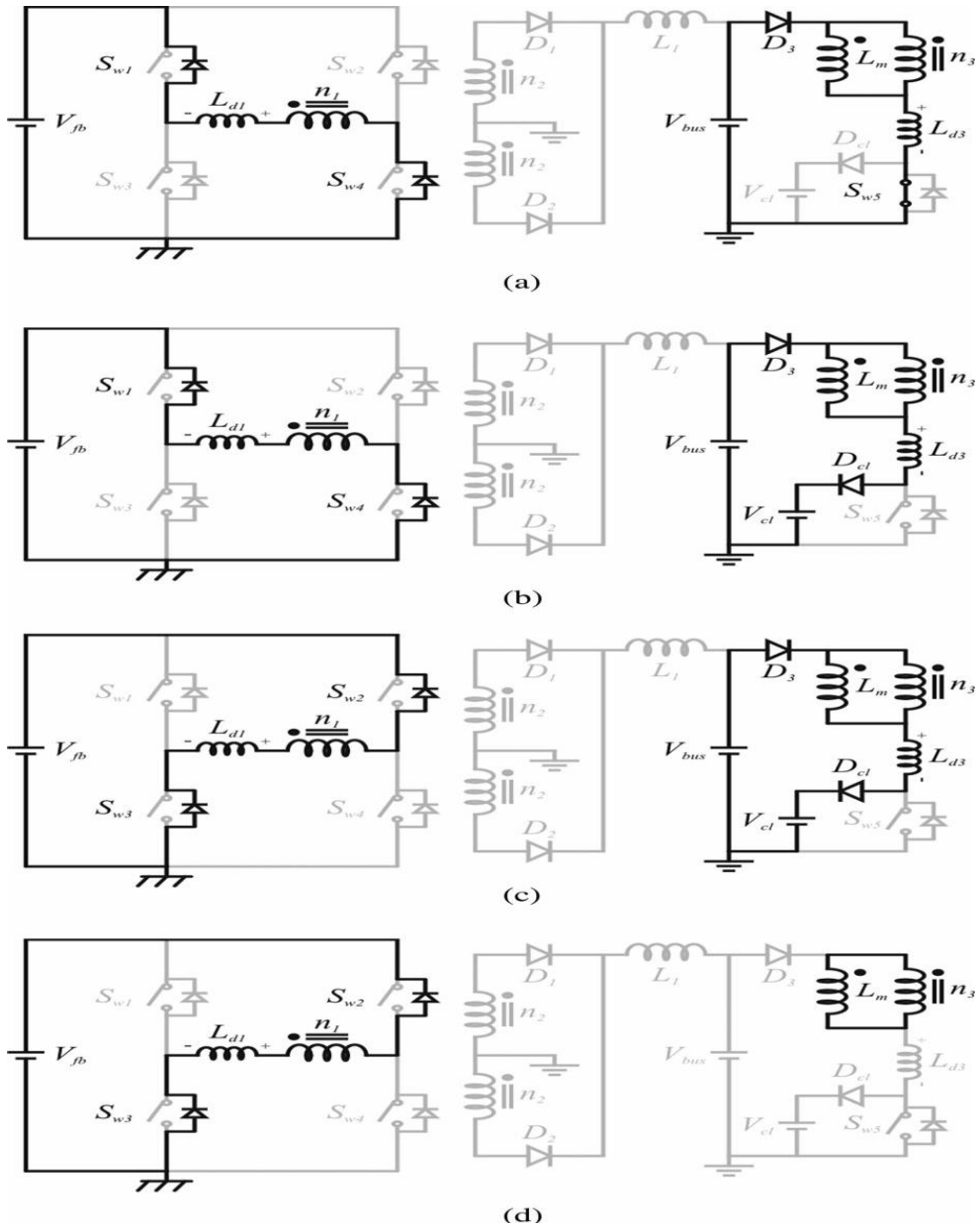

Figure.4: Operation stages of the proposed converter with passive clamping:

(a) first stage, (b) second stage, (c) third stage, and (d) fourth stage

First Stage: This stage, shown in Fig. 10(a), starts when the forward converter switch *Sw*5 is turned ON. The antiparallel diodes of the *Sw*1 and *Sw*4 switches also turn ON once they are forward biased. Positive voltages are applied to the transformer magnetizing (1) and primary (2) and tertiary (3) leakage inductances.

Therefore, the currents through these elements increase

$$V_{Lm} - 1(t) = \frac{L_m\left(n^2 L_{di} V_{bus} + nV_{fb} V_{d3}\right)}{n^2 L_{d1}(L_m + L_{d3}) + L_m L_{d3}} \qquad (\mathbf{1})$$

$$V_{Ld1-}(t) \quad = \frac{V_{Lm-(t)}}{n} - V_{fb} \qquad (2)$$

$$V_{\ Ld3-}1(t) = V_{bus} \quad - V_{Lm-1}(t) \qquad (3)$$

Second Stage: This stage, shown in Fig. 10(b), starts when the forward converter switch turns OFF. Therefore, the clamping diode *D*cl turns ON, assuming the current that circulated through the forward converter switch.

This current decreases because a negative voltage (4) is applied to the tertiary winding leakage inductance. The currents through the antiparallel diodes of the *Sw*1 and *Sw*4 switches also decrease because the voltage applied to the primary winding leakage inductance (5) becomes negative. In this subinterval, the magnetizing current is deviated to the clamping circuit, resulting in losses for the topology. The clamping circuit voltage causes overvoltage on the forward converter switch; however, a high value reduces the duration of this and the next stages, reducing the clamping circuit losses. The voltage across the magnetizing inductance is given by (4)

$$V_{Ld3\_}2(t) = V_{bus} - V_{cl} - V_{Lm} - 2(t) \qquad (4)$$

$$V_{Ld1\_}2(t) = \frac{V_{Lm\_}2(t)}{n} - V_{fb} \qquad (5)$$

$$V_{Lm-2}(t) = \frac{L_m\left(n^2 L_{d1(V_{bus}\_V_{cl})} + nV_{fb}L_{d3}\right)}{n^2 L_{d1(L_m+L_{d3})} + L_{mL_{d3}}} \qquad (6)$$

Third Stage: This stage, shown in Fig. 10(c), starts when the antiparallel diodes of the *Sw*1 and *Sw*4 switches turn OFF, since the current through them reaches zero, and the antiparallel diodes of the *Sw*2 and *Sw*3 switches turn ON. The current through these diodes increases because the voltage applied to the primary winding leakage inductance (7) continues negative. Therefore, the current through the primary winding is inverted. The current through the clamping circuit diode continues to decrease once the voltage applied to the tertiary winding leakage inductance (8) keeps negative, but with a lower rate. Therefore, in this subinterval, the magnetizing current is gradually transferred from the clamping circuit to the converter output. The voltage across the magnetizing inductance is given by (9)

$$V_{Ld1\_}3(t) = \frac{V_{Lm\_}3(t)}{n} + V_{fb} \qquad (7)$$

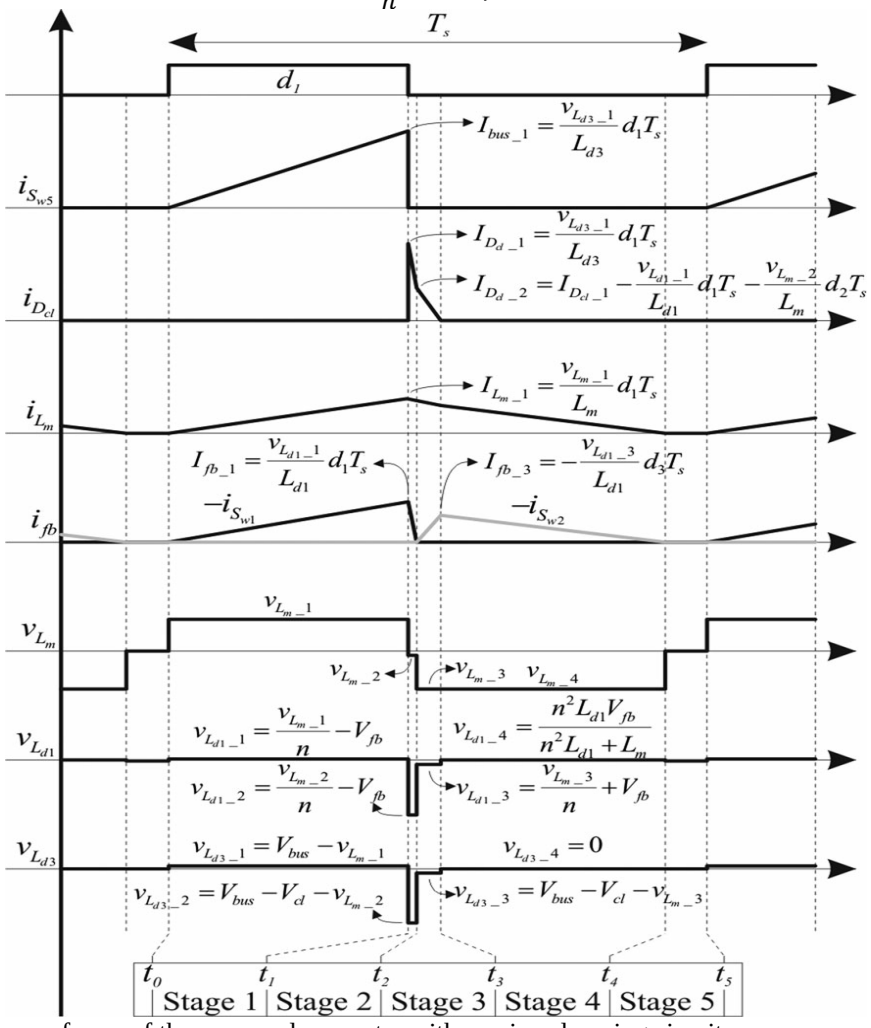

Figure.5.: Main waveforms of the proposed converter with passive clamping circuit.

$V_{Ld3\_}3(t) = V_{bus} - V_{cl} - V_{Lm} - 3(t$ (8))

$$V_{Lm-3}(t) = \frac{L_m\left(n^2 L_{d1(V_{bus}-V_{cl})} - nV_{fb}L_{d3}\right)}{n^2 L_{d1(L_m+L_{d3})} + L_m L_{d3}} \qquad (9)$$

the current through the clamping circuit diode *D*cl reaches *Fourth Stage:* This stage, shown in Fig. 4(d), starts when zero and it turns OFF. The currents through the antiparallel diodes the *Sw*2 and *Sw*3 switches decrease once the voltage applied to the primary winding leakage inductance (10) becomes positive. The voltage applied to the tertiary winding leakage inductance (11) is equal to zero and applied to the magnetizing inductance is given by (12)

$$V_{Ld1-}4(t) = \frac{n^2 L_{d1} V_{fb}}{n^2 L_{d1} + L_m} \qquad (10)$$

$$V_{Ld3-}4(t) = 0 \qquad (11)$$

$$V_{Ldm-}4(t) = \frac{nL_{d1} V_{fb}}{n^2 L_{d1} + L_m} \qquad (12)$$

Fifth Stage: This stage starts when the antiparallel diodes of the *Sw*2 and *Sw*3 switches turn OFF once the current through them reaches zero. The voltages applied to the primary and tertiary windings leakage inductances, and converter current are equal to zero. This stage ends when the forward converter switch *Sw*5 is turned ON, starting the next operation period.

Fig. 11 shows the main waveforms of the converter operating in discontinuous conduction mode. These waveforms are forward converter switch current *iSw*5 , clamping circuit diode current *i*Dcl , magnetizing inductance current *iLm*, output current *i*fb , voltages across the magnetizing inductance *vLm*, and primary *vLd*1 and tertiary *vLd*3 winding leakage inductances. The respective subintervals are also indicated.

This topology solves the voltage spike problem. However, during the clamping circuit on state, the magnetizing inductance current is deviated toward the passive elements. This process imposes power losses on the topology, which reduce the converter efficiency. A similar magnetizing current deviation also happens in flyback converter.

III. Transformer Design Methodology

This section presents a design methodology for the transformer of the proposed full-bridge-forward integrated converter including a bidirectional converter, based on the parameters shown in Table II. The full-bridge charging voltage is the voltage level that should be present after the full bridge converter in order to charge the energy storage system.

The full-bridge discharging voltage is the voltage level present between the bidirectional converter and the full-bridge converter in the discharging process.

The turns ratio *n*2 /*n*1 between the primary and secondary transformer windings must be such that it allows the voltage boost from the bidirectional converter of the energy storage system voltage level *V*fb to the dc bus voltage level *V*bus, so that

$$\frac{n_2}{n_1} > \frac{V_{bus}}{V_{fb}} \cdot \frac{1}{D_{ef}} \qquad (13)$$

where *D*ef is the effective full-bridge converter duty cycle. For the adopted converter parameters and assuming *D*ef equal to 0.85, this relation must be higher than 5.5.

On the other hand, the turns ratio *n*3 /*n*1 between the tertiary and primary transformer windings must be lower than the relation between *V*bus and *V*charg in order to allow the storage system charging process, then

$$\frac{n_3}{n_1} < \frac{V_{bus}}{V_{charg}} \cdot \frac{1}{D_{ef}} \qquad (14)$$

For the adopted converter parameters, this relation must be lower than 8; otherwise, the voltage across the energy storage system does not reach 50 V needed for the charging process.

In addition, the turns ratio *n*3 /*n*1 between the tertiary and primary transformer windings must also be such that the sum between the reflected tertiary voltage on full-bridge converter operation and the dc bus voltage is lower than the maximum forward converter switch breakdown voltage *VSw*5 max, once this voltage is applied across the clamping circuit capacitor.

Therefore, this turns ratio must respect (15) and, for the adopted converter parameters, it must be lower than 8.42

$$\frac{n_3}{n_1} < \frac{V_{S_{w-5}} - V_{bus}}{V_{fb}} \qquad (15)$$

The turns ratio *n*3 /*n*2 between the tertiary and secondary transformer windings must respect (16) to prevent current circulation through the diodes of the secondary bridge during the forward converter operation stages in which a negative voltage is applied across the tertiary winding

$$\frac{n_3}{n_2} < \frac{V_{cl} - V_{bus}}{V_{cl}} \qquad (16)$$

If this ratio is lower than 1, the upper diode *D*1 starts to conduct (*n*2–*D*1–*L*1–*V*bus) and if (16) is not satisfied, the bottom diode *D*2 starts to conduct (*n*2–*D*2–*L*1–*V*bus), resulting in additional power losses, but which are very low due to the small current value. For the adopted converter parameters, this relation must be higher than 1.25.

Taking into account that the proposed converter must operate under the residential microgrid power, voltage, and current parameters, which are shown in Table II, to achieve proper operation, the transformer turns ratio must follow the relation

$$1 < \frac{n_2}{n_1} < \frac{n_3}{n_1} < 8 \qquad (17)$$

The transformer has great importance in the converter performance, as it influences the converter efficiency not only due to its inherent losses, but also due to the clamping circuit losses depending on the magnetizing and leakage inductances. Therefore, careful attention should be paid to its design. Taking into account the presented design methodology, the chosen transformer turns ratio is *n*1 = 1, *n*2 /*n*1 = 6, and *n*3 /*n*1 = 7.

TABLE II Converters, Comparison

Parameters	DAB	DAB + bidirectional	FB-Forward + bidirectional
Active switches	8	10	7 or 8 (with active clamping)
Inductors	0	1	2
Diodes	0	0	4
RMS input (storage) current (A)	32.71	29.53	29.31
Input current ripple (A)	63.89	3.93	3.82
RMS output (DC bus) current (A)	5.45	3.96	3.50
Output current ripple (A)	16.61	7.40	0.45
RMS primary current (A)	32.71	23.73	22.01
RMS secondary current (A)	5.45	3.96	3.45
Transformer turns ratio	1:6	1:6	1:6:7
Transformer core volume (cm^3)	78.20	78.20	78.20
Transformer leakage inductance (μH)	4	6.67	1
Phase-shift angle (degrees)	41	41	161
Bidirectional converter RMS switch currents (A)	-	22.85	22.69
Primary full-bridge RMS switch currents (A)	23.58	16.79	18.67
Secondary full-bridge RMS switch currents (A)	3.91	2.80	-
Primary full-bridge switch voltage (V)	48	80	80
Secondary full-bridge switch voltage (V)	400	400	-

The DAB with a bidirectional converter presents high output current ripple and demands ten semiconductor switches. Regarding the proposed converter, the RMS input, output, and transformer currents are similar, but lower than its counterparts, demanding less parallel wires. The RMS switches' currents are also similar, demanding practically the same devices' current levels. Therefore, it can be concluded that low input and output current ripples are achieved with less or the same number of active devices, without compromising the transformer volume and the switches current levels.

IV. Experimental Results

This section presents some experimental results of the fullbridge converter, which is responsible for the energy storage system discharging process, and of the double-ended forward converter without an output inductor originated from the proposed integration process, which is responsible for the energy storage system charging process. The bidirectional convenot inserted. The three studied forward converter clamping circuits are approached.

Due to the presence of the full-bridge converter for the discharging process, the input voltage of a system is 12V.And it is boost up to 48V using boost converter. and the output of Full bridge converter is 400V. And DC bus voltage is 400.Full bridge charging voltage is 50 to 55V.Full bridge discharging voltage is 80V.Nominal storage system voltage is 48V.Nominal charging power is 100W.Minimum storage system voltage is 24V

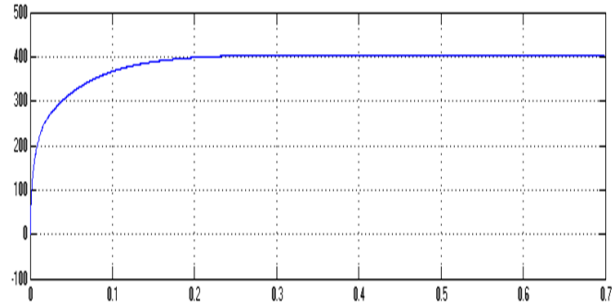

Figure.3: output voltage of open loop system

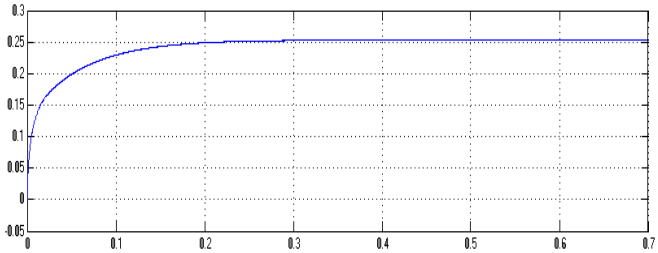

Figure.4.: output current of open loop system

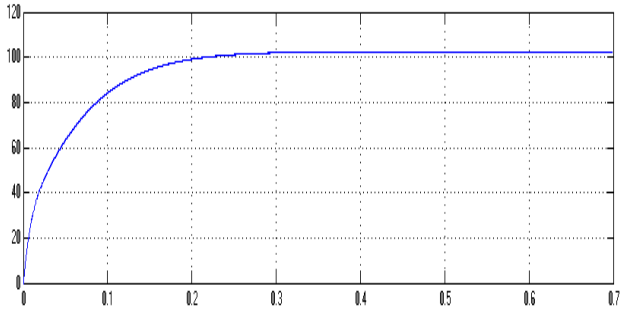

Figure.5: output power of open loop system

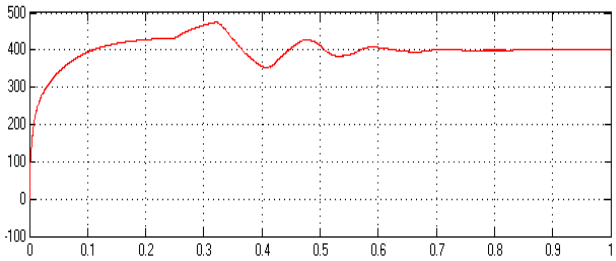

Figure.6.:output voltage of closed loop system

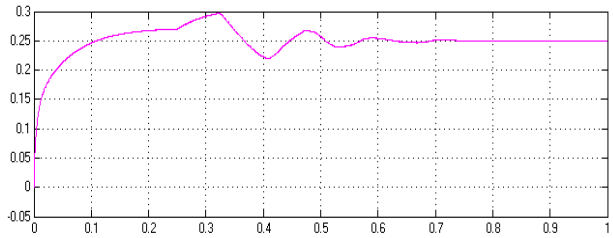

Figure.7.output current of closed loop system

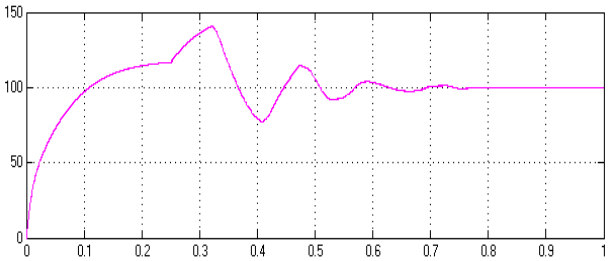

Figure.8: output power of closed loop system.

V. Conclusion

This project has presented the procedures for the Full-Bridge-Forward DC–DC Converter for a Residential Micro grid Application system. This project proposes an integrated full-bridge-forward dc–dc converter to connect the energy storage system to the dc bus of a residential micro grid and high usage of the super capacitor bank stored energy, and a long battery bank lifetime. The proposed topology presents low input and output current ripple, high voltage ratio, high power operation on the discharging process, galvanic isolation, and bidirectional power flow. This project is focused on the double-ended forward converter originated from the integration process. The integration process practically does not affect the full-bridge converter efficiency.

The simulation circuits are developed using elements of simulink library. The Simulation is successfully done and open loop / closed loop simulation results are presented. Results are verified through numeric simulation using mat lab.

REFERENCES

[1] K. Sun, L. Zhang, Y. Xing, and J. M. Guerrero, "A distributed control strategy based on DC bus signaling for modular photovoltaic generation systems with battery energy storage," *IEEE Trans. Power Electron.*, vol. 26, no. 10, pp. 3032–3045, Oct. 2011.

[2] F. A. Farret and M. G. Sim˜oes, *Integration of Alternative Sources of Energy*, 1st ed. New Jersey: Wiley, 2006.

[3] Y. A.-R. I. Mohamed, "Mitigation of converter-grid resonance, grid induced distortion, and parametric in stabilities in converter-based distributed generation," *IEEE Trans. PoWer Electron.*, vol. 26, no. 3, pp. 983– 996, Mar. 2011.

[4] R. H. Lasseter and P. Paigi, "Microgrid: A conceptual solution," in *Proc. IEEE Power Electron. Spec. Conf.*, Jun. 2004, vol. 6, pp. 4285–4290.

[5] H. Zhou, T. Bhattacharya, D. Tran, T. S. T. Siew, and A. M. Khambadkone, "Composite energy storage sy stem involving battery and ultra capacitor with dynamic energy management in microgrid applications," *IEEE Trans. Power Electron.*, vol. 26, no. 3, pp. 923–930, Mar. 2011.

[6] J.-Y. Kim, J.-H. Jeon, S.-K. Kim, C. Cho, J. H. Park, H.-M. Kim, and K.-Y. Nam, "Cooperative control strategy of energy storage system and microsources for stabilizing the microgrid during islanded operation," *IEEE Trans. Power Electron.*, vol. 25, no. 12, pp. 3037–3048, Dec. 2010.

[7] R. S. Balog and P. T. Krein, "Bus selection in multibus DC microgrids," *IEEE Trans. Power Electron.*, vol. 26, no. 3, pp. 860–867, Mar. 2011.

[8] J. Chen, J. Chen, R. Chen, X. Zhang, and C. Gong, "De -coupling control of the non-grid-connected wind power sy - stem with the droop strategy based on a DC micro-grid," in *Proc. World Non-Grid-Connected Wind Power Energy Conf.*, 2009, pp. 1–6.

[9] L. Roggia, C. Rech, L. Schuch, J. E. Baggio, H. L. Hey, and J. R. Pinheiro, "Design of a sustainable residential microgrid system including PHEV and energy storage device," in *Proc. Eur. Conf. Power Electron. Appl.*, 2011, pp. 1–9.

[10] F. Ongaro, S. Saggini, and P. Mattavelli, "Li-ion ba -ttery-supercapacitor hybrid storage system for a long life time, photovoltaic-based wireless sensor network," *IEEE Trans. Power Electron.*, vol. 27, no. 9, pp. 3944–3952, Sep. 2012.

[11] J. Cao and A. Emadi, "A new battery/ultracapacitor hybrid energy storage system for electric, hybrid, and plug-in hybrid electric vehicles," *IEEE Trans. Power Electron.*, vol. 27, no. 1, pp. 122–132, Jan. 2012.

[12] H. Zhou and A. M. Khambadkone, "Hybrid modulation for dual-activebridge bidirectional converter with extended power range for ultracapacitor application," *IEEE Trans. Ind. Appl.*, vol. 45, no. 4, pp. 1434–1442, Jul. 2009.

[13] F. Krismer and J. W. Kolar, "Closed form solution for minimum conduction loss modulation of DAB converters," *IEEE Trans. Power Electron.*, vol. 27, no. 1, pp. 174–188, Jan. 2012.

[14] D.Vinnikov, I. Roasto, and J. Zakis, "Newbi-directionalDC/DC converter for supercapacitor interfacing in high-power applications," in *Proc. Int. Power Electron. Motion Control Conf.*, 2010, pp. T11-38–T11-43.

[15] K. Wang, F. C. Lee, and J. Lai, "Operation principles of bi-directional full-bridge DC/DC converter with unified soft-switching scheme and soft starting capability," in *Proc. IEEE Appl. Power Electron. Conf.*, 2000, vol. 1, pp. 111–118.

[16] L. Corradini, D. Seltzer, D. Bloomquist, R. Zane, D. Maksimovic, and B. Jacobson, "Minimum current operation of bidirectional dual-bridge series resonant DC/DC converters," *IEEE Trans. Power Electron.*, vol. 27,no. 7, pp. 3266–3276, Jul. 2012.

[17] Z. Zhang, Z. Ouyang, O. C. Thomsen, and M. A. E. Andersen, "Analysis and design of a bidirectional isolated DC–DC converter for fuel cells and supercapacitors hybrid system," *IEEE Trans. Power Electron.*, vol. 27, no. 2, pp. 848–859, Feb. 2012.

[18] N. M. L. Tan, T. Abe, and H. Akagi, "Design and performance of a bidirectional isolated DC–DC converter for a battery energy storage system," *IEEE Trans. Power Electron.*, vol. 27, no. 3, pp. 1237–1248, Mar. 2012.

[19] M. N. Gitau, G. Ebersohn, and J. G. Kettleborough, "Power processor for interfacing battery storage system to 725 V DC bus," *Energy Convers. Manage.*, vol. 48, no. 3, pp. 871–881, Mar. 2007.

[20] M. Nowak, J. Hildebrandt, and P. Luniewski, "Converters with AC transformer intermediate link suitable as interfaces for supercapacitor energy storage," in *Proc. IEEE Power Electron. Spec. Conf.*, Jun. 2004, vol. 5, pp. 4067–4073.

[21] H. Tao, A. Kotsopoulos, J. L. Duarte, and M. A. M. Hendrix, "Multiinput bidirectional DC–DC converter combining DC-link and magneticcoupling for fuel cell systems," in *Proc. IEEE Ind. Appl. Conf.*, Oct. 2005, vol. 3, pp. 2021–2028.

[22] H. Tao, J. L. Duarte, andM. A.M. Hendrix, "Three-port triple-half-bridge bidirectional converter with zero-voltage switching," *IEEE Trans. Power Electron.*, vol. 23, no. 2, pp. 782–792, Mar. 2008.

[23] G. Chen, Y.-S. Lee, D. Xu, and Y. Wang, "A novel soft-switching and low-conduction-loss bidirectional DC–DC converter," in *Proc. Int. Power Electron. Motion Control Conf.*, 2000, vol. 3, pp. 1166–1171

[24] F. G. Capponi, P. Santoro, and E. Crescenzi, "HBCS converter: A bidirectional DC/DC converter for optimal power flow regulation in supercapacitor applications," in *Proc. IEEE Ind. Appl. Conf.*, Sep. 2007, pp. 2009–2015.

[25] M. H. Todorovics, L. Palma, and P. N. Enjeti, "Design of a wide input range DC–DC converter with a robust power control scheme suitable for fuel cell power conversion," *IEEE Trans. Ind. Electron.*, vol. 55, no. 3,pp. 1247–1255, Mar. 2008.

[26] S.-J. Jang, T.-W. Lee, W.-C. Lee, and C.-Y. Won, "Bi-directional dc–dc converter for fuel cell generation system," in *Proc. IEEE Power Electron. Spec. Conf.*, Jun. 2004, vol. 6, pp. 4722–4728.

[27] M. B. Camara, H. Gualous, F. Gustin, and A. Berthon, "Design and new control of DC/DC converters to share energy between supercapacitors and batteries in hybrid vehicles," *IEEE Trans. Veh. Technol.*, vol. 57, no. 5, pp. 2721–2735, Sep. 2008.

[28] T. C.Wang, Z. H. Ye, G. Sinha, and X. M. Yuan, "Output filter design for a grid-interconnected three-phase inverter," in *Proc. IEEE Power Electron. Spec. Conf.*, Acapulco, Mexico, Jun. 2003, pp. 779–782.

[29] C.-L. Chen, Y. Wang, J.-S. Lai, Y.-S. Lee, and D. Martin, "Design of parallel inverters for smooth mode transfer microgrid applications," *IEEE Trans. Power Electron.*, vol. 25, no. 1, pp. 6–15, Jan. 2010.